

Review of 2011 Preese Hall Well Stimulations and

Proposed Alternate Stimulation Method for UK Bowland-Hodder Shale Gas

Executive Summary:

GeoSierra conducted a recent extensive in-house review of the 2011 Preese Hall well stimulations of the Bowland-Hodder shales, and from that review developed a proposed alternate method of well stimulation in the UK Bowland-Hodder shales.

During the Preese Hall well stimulations, the bedding planes were opened by the high net fracturing pressures and lead to extremely high leak-off and very low fracture fluid efficiency, both contrary to what would be required to enhance production in a nano-Darcy shale. A high frequency of low friction angle 6° slickensided bedding planes dipping at 30°, and thin clay rich bands, fault gouge, parallel or subparallel to bedding, were encountered in the Preese Hall core. These features impeded the vertical growth of hydraulic fractures. Once the hydraulic fractures vertical growth is stopped, the net fracturing pressures rise to allow the fracturing fluid to enter and flow along the hyper-stress sensitive bedding planes, thus giving rise to a heightened risk of induced seismicity and minimal enhanced gas production.

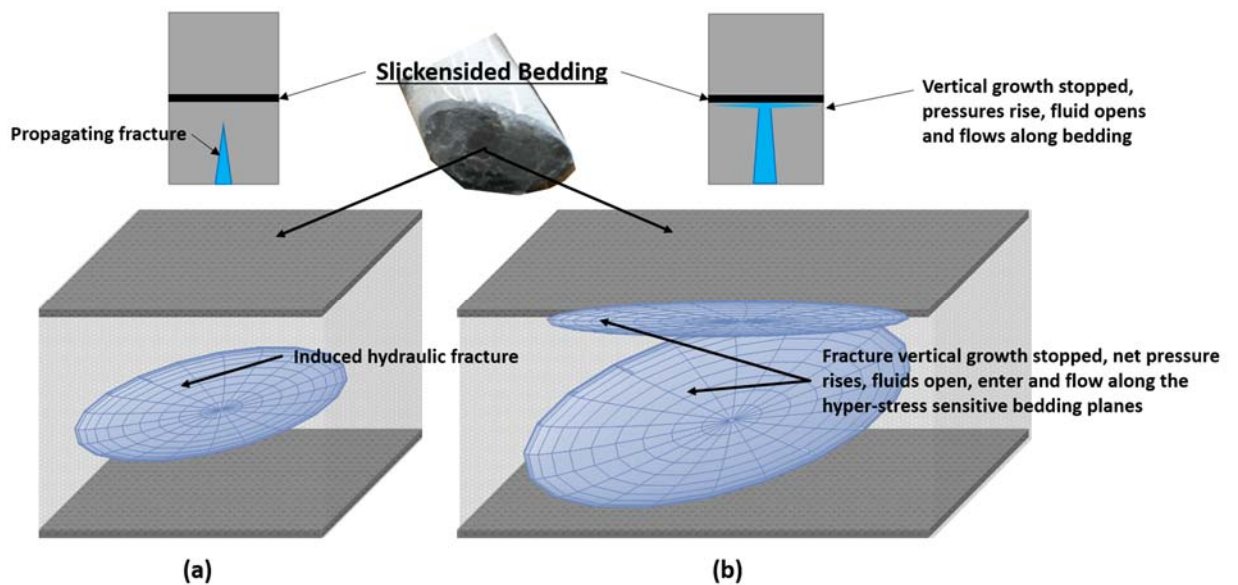


Figure 1. a) Initiated and propagating hydraulic fracture, b) fracture vertical growth impeded, net pressure rises, fluids enter and flow along the hyper-stress sensitive bedding planes.

For example, a hydraulic induced fracture in the stiff Bowland shale under strike-slip stress state can't propagate vertically through the slickensided bedding surfaces and the thin clay rich bands as detected throughout the core in the Preese Hall well at the stimulation depths. From data on stress state estimates and strength of these slickensided bedding planes and thin clay rich bands, a validated numerical model computed that the induced hydraulic fracture will terminate in height growth, net pressure will rise and the fracturing fluid open and flow along the hyper-stress sensitive bedding planes resulting in the high net pressures observed. The bedding planes being hyper-sensitive to stress will yield extremely high leak-off and extremely low fracture fluid efficiency – all features experienced in all of the Preese Hall stimulations.

Due to the hyper-stress sensitivity of the bedding plane hydraulic conductivity to effective stress, significantly elevated pore pressures $\sim 2,500$ psi were computed some 1,700' away from the stimulated well, during and after the stage 2 stimulations with a small time lag experienced during injection. The stimulations gave rise to fifty two (52) seismic events $> M_L 0$, all of which had similar waveforms and were in close proximity to the two largest induced events of $M_L 2.3$ and $M_L 1.5$, whose hypocenter was estimated to be $\sim 1,200'$ east of the stimulated well.

It is envisaged and supported by preliminary analyses, that if a sufficiently large (i.e. high) vertical fracture is initiated and generated either at or close to the stimulated wellbore, then this vertical fracture will propagate laterally, irrespective of the slickensided bedding planes, at low net fracturing pressures. The objective of the stimulation procedure is to create a long and high induced vertical fracture with minimal leak-off, that has a high probability of significant enhanced gas production, whilst minimizing the risk of induced seismicity.

Current perceived methods to achieve such a high height growth fracture at or close to the stimulated wellbore are shown in the figure below, being:

- a) complex completion of split casing and dilated expanded inner slotted liner, to initiate vertical fracture, simple pumping schedule, brute force approach, perceived as low risk,
- b) orientated slots formed by jetting or shaped charges, with the oriented slots reducing breakdown pressures, modified pumping schedule to achieve coalesced height growth of the induced hydraulic fractures, perceived as moderate risk, and
- c) orientated perforations, with complex pumping schedule to achieve multiple breakdowns with minimal fracture growth, followed by fracture growth to achieve coalesced height growth of the induced hydraulic fractures, perceived as high risk.

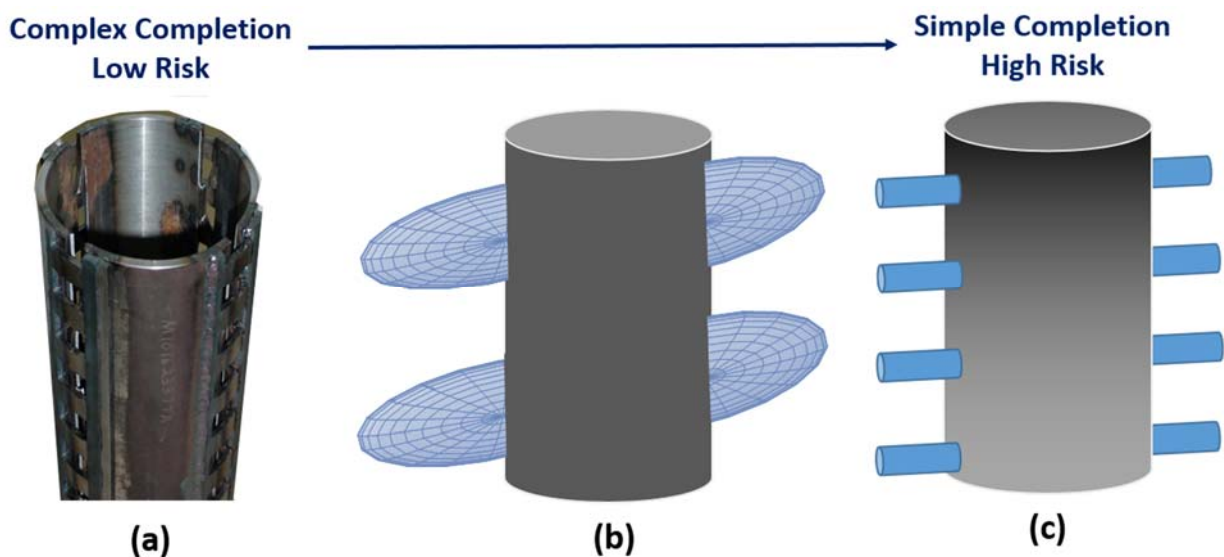


Figure 2. Current perceived stimulation methods a) sleeve initiated fracture - low risk, b) orientated slots by jetting or shape charges - moderate risk, and c) orientated perforations - high risk.

Background USA and Canada:

The interaction of hydraulic induced fractures with existing natural fractures has been studied in detail in the laboratory, and in the field by a process of trial and error. Un-bonded weak bedding planes have been known for decades from mined back experiments to stop hydraulic fracture vertical growth, Warpinski et al. (1981). Two different field examples are summarized for the USA Bakken and the Barnett shales.

For example; in the Bakken, the shale rocks are too ductile to induce a fracture by fluid pressure, so vertical hydraulic fractures are induced by hydraulic fracturing the elastic brittle neighboring rocks. These fractures propagate upwards through the interface and induce a vertical fracture in the shales. The interface is sufficiently strong to induce tensile stresses in the shale and thus the fracture propagates upwards into the shale.

In the Barnett, being an elastic strong brittle shale, fractures are induced hydraulically in the shale that propagate and connect to existing fractures and due to the limited length of the natural fractures, induced fractures are formed at the end of the natural fracture, as shown in the figure below taken from Gale et al. (2007).

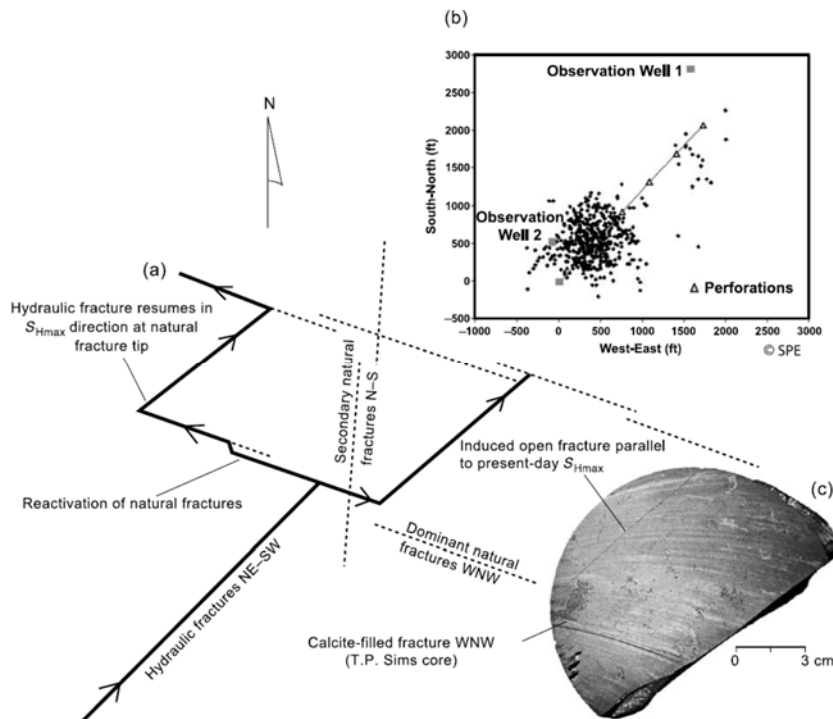


Figure 1. Diagrammatic representation of hydraulic fracture and natural fracture interaction in the Barnett shale. (a) Hydraulic fracture NE-SW activates natural fracture WNW-ESE and secondary natural fracture N-S, (b) map of microseismic data and (c) core containing hydraulic and natural fractures – taken from Gale et al. (2007).

Whether a hydraulic induced fracture on intersection with a natural fracture, crosses the natural fracture unimpeded or terminates and activates the natural fracture as shown below, depends on a number of

parameters; namely, angle between the fractures, stiffness and strength of the natural fracture, propagation rate of the hydraulic fracture, stiffness and anelasticity of the rocks either side of the natural fracture, stress state, and leakoff coefficients in both the rock and natural fracture. An illustration of the intersection of a hydraulic induced fracture interacting with a natural fracture is shown below, from Blanton (1982).



Figure 2a. Propagating hydraulic fracture crosses the natural fracture and keeps propagating without any significant change. Left is a schematic and right is experimental study from Blanton (1982).

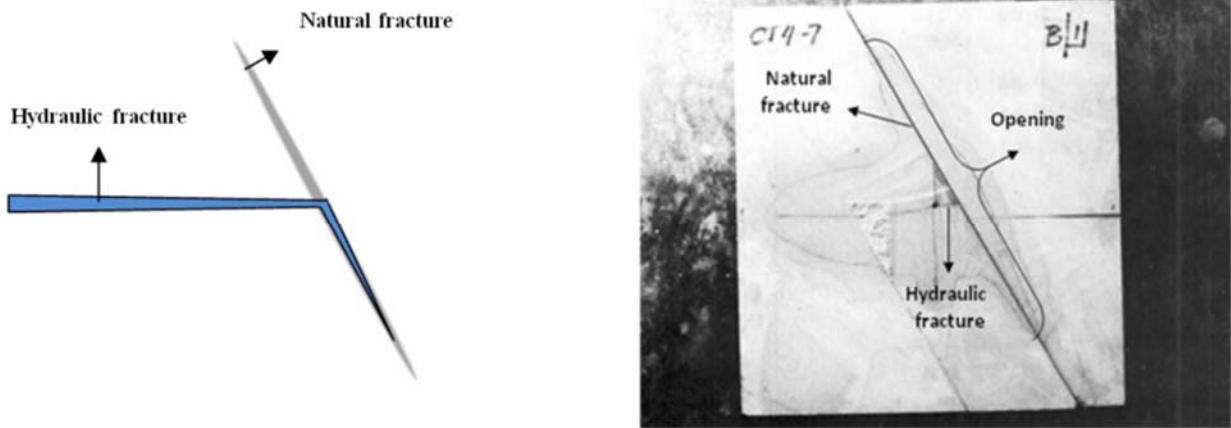


Figure 2b. Propagating hydraulic fracture turns into the natural fracture and propagates along it. Left is a schematic and right is experimental study from Blanton (1982).

If the hydraulic fracture turns into and activates the natural fracture, then the probability of whether a new induced hydraulic fracture is generated as in the Barnett shale, depends on the rock anelasticity, the natural fracture properties, stiffness, strength, leak off and termination properties, pumping rate and leak-off.

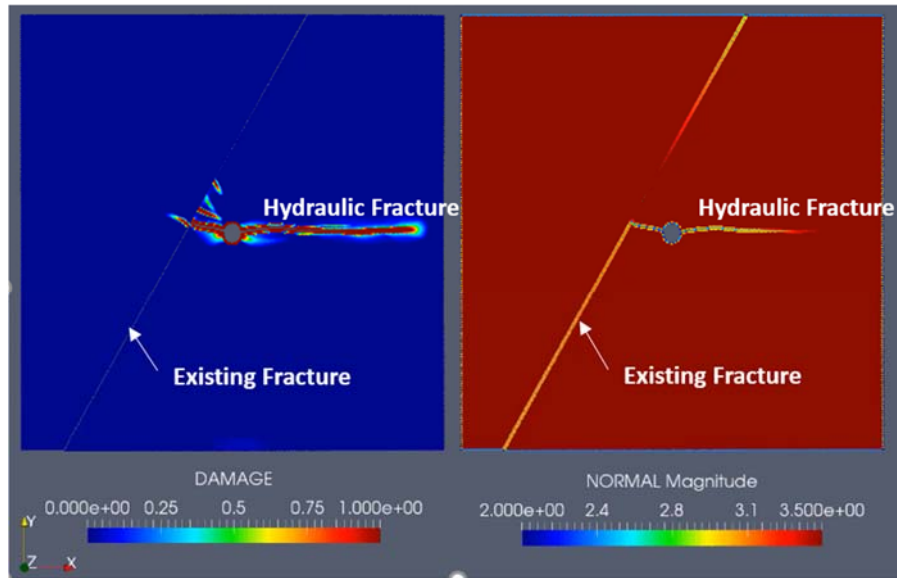


Figure 3. Validated model analysis of experimental data on the propagation of a hydraulic fracture and its interaction with an existing nature fracture. In this case the hydraulic fracture turns into, opens and propagates along the natural fracture.

The anelasticity of the stimulated formation has been shown, Hocking et al. (2013), to be the prime parameter whether a formation can be hydraulically fractured by fluid pressure alone. In the Milk River tight gas reservoir, comparison of offset wells stimulated through perforations and dilated casings respectively have shown conclusively from pressure measurements, surface and downhole tiltmeters that in such formations hydraulic induced features stimulated through perforations do not form fractures. The hydraulically induced features do not follow the propagating path of least dissipating energy state, i.e. are not normal to the minimum principal stress, and are either cavity expansions in weak formations or horizontal features in stronger formations indicating that the vertical stress is a minimum when in fact it is not.

USA experience of stimulating deep clay rich low perm turbidite formations has shown that stimulating these formations by fluid injection through perforations does not enhance production and in fact produces horizontal features contrary to the insitu stress state.

Onshore UK

The sedimentary basins in the UK considered for stimulation are the Weald basin in the south of England, the Bowland, Blacon, Gainsborough, Widerpool, Edale and Cleveland basins in the middle of England and the Midland Valley basin in Scotland. The formations considered for stimulation vary from clay rich source shale in the Weald, strong stiff brittle and clay rich source shales, mudstones, grits, and turbidites in the middle of England and clay rich source shales in the Midland Valley basin. The formations of interest are either more anelastic than those stimulated in the USA and Canada, or in the case of the stiff strong brittle Bowland shale formations, that were stimulated, have a high frequency of both significantly weak slickensided bedding planes and thin clay rich bands, parallel or subparallel to bedding, contained within them.

Review of 2011 Preese Hall Well Stimulations

A recent in-house review was completed of the Preese Hall well stimulations, from available literature, de Pater and Baisch (2011), Baker-Hughes (2011), Baisch and Voros (2011), Eisner et al. (2011), de Pater and Pellicer (2011), Eisner et al. (2013), Clarke et al. (2014) and the DECC report by Green et al. (2012).

It is clear from this review that there has been a lack of appreciation of the differences in the geology and material properties of the formations in the Bowland basin compared to successful stimulations in the USA and Canadian shales, and also a lack of insight into the experience and expertise from the USA and Canada of stimulating low perm turbidites and tight mudstones that experience anelastic behaviour. That is, the induced hydraulic fracture does not always propagate in the path of the least energy dissipating state, especially due to the presence of existing fractures, anelastic behaviour and low friction slickensided bedding planes.

Weak un-bonded bedding planes have been known for some time to stop vertical growth of hydraulic fractures, Warpinski et al. (1981), as shown in Figure 4 of a mined back field experiment. The hydraulic fracture tip blunts at the interface, fracturing pressures rise and the hydraulic fracture widens at the interface, and in the case of Figure 4, the fracture propagated downwards as its upward vertical growth was stopped by and at the weak interface.

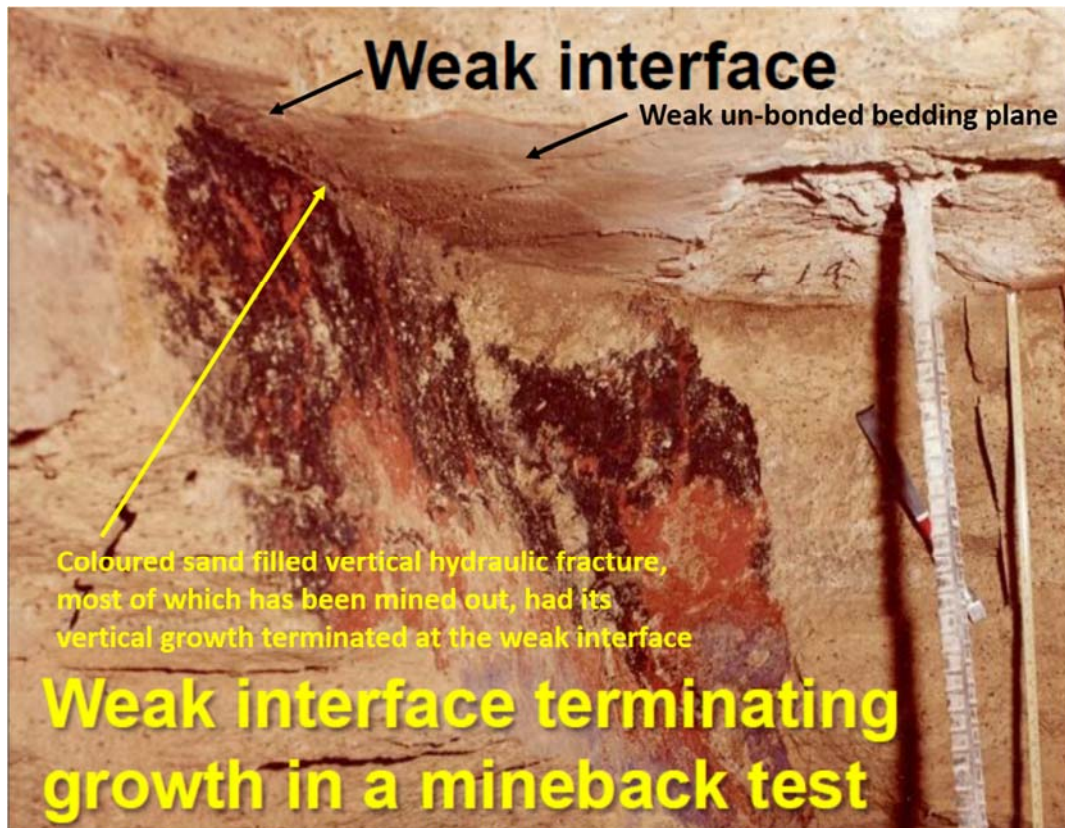


Figure 4. Mined back photograph of a weak un-bonded bedding plane terminating vertical growth of a hydraulic fracture, after Fisher and Warpinski (2011) from field experiments of Warpinski et al. (1981).

A high frequency of weak low friction 6° slickensided bedding planes, dipping at 30°, were encountered throughout the Preese Hall core, as shown in Figure 5. Fifteen (15) slickensided bedding planes at 30° dip

were recorded at measured depths greater than 8,000' MD, and were also encountered at high frequency at shallower depths, de Pater and Baisch (2011). Thin clay rich bands, referred to as fault gouge, parallel or subparallel to bedding, were encountered throughout the Preese Hall core, with an especially high frequency in the Hodder Mudstone formation at 8,480', 8,505', 8,560', 8,575', 8,605', 8,610', 8,620', 8,630' and 8,640' MD, de Pater and Baisch (2011).



Figure 5. High frequency of slickensided bedding planes dipping at 30° were encountered throughout the Preese Hall core, left at 6,835' MD and right at 8,185' MD, taken from de Pater and Baisch (2011).

The high frequency of slickensided bedding planes dipping at 30° and thin clay rich bands, parallel or subparallel to bedding, both of very low frictional strength of $\phi=6^\circ$ de Pater and Baisch (2011), impeded the vertical growth of hydraulic induced vertical fractures, that were initiated in the stiff elastic brittle shale by fluid injection through perforations. The hydraulic fracture vertical growth was stopped by these features, resulting in a rise of the net fracturing pressure, to allow the fracturing fluid to open and flow along the hyper-stress sensitive bedding planes, as shown in Figure 6, heightening the risk of induced seismicity with minimal enhanced gas production.

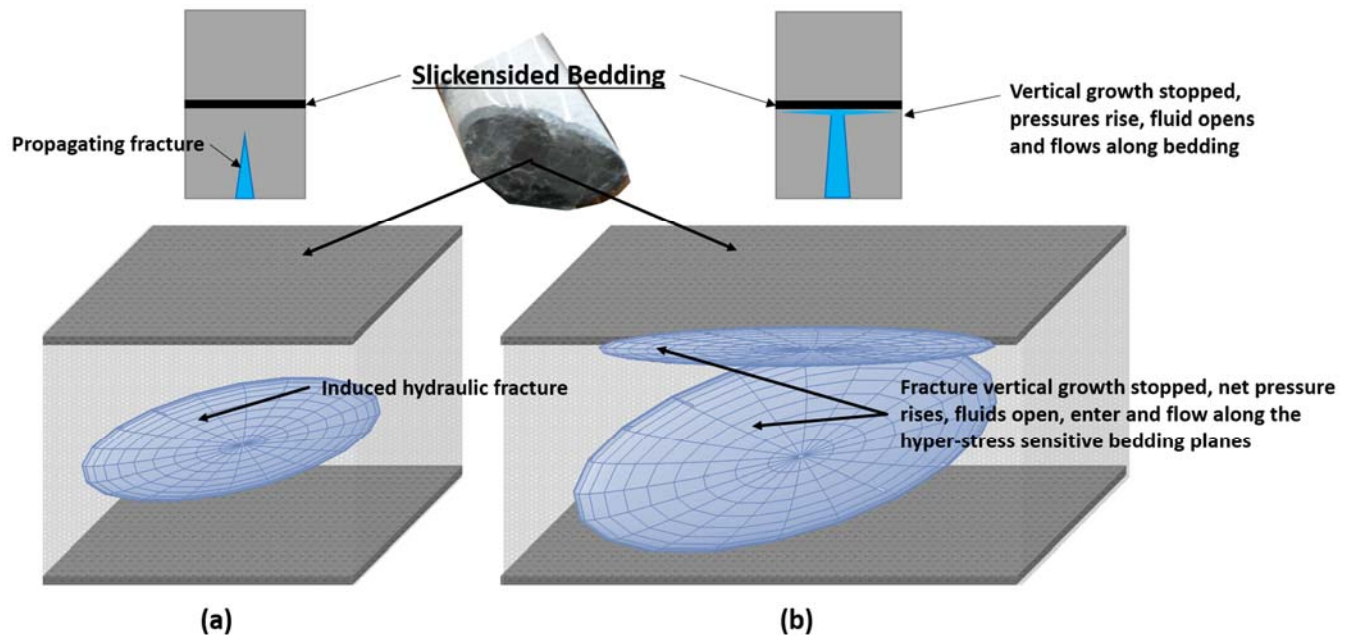


Figure 6. a) Initiated and propagating hydraulic fracture, b) fracture vertical growth impeded, net pressure rises, fluids enter and flow along the hyper-stress sensitive bedding planes.

The Presse Hall well completion is shown in Figure 7. The 5-1/2" casing was perforated at the depths shown with twenty seven (27) shots per each 9' interval. Each zone was stimulated as stages, first a minifrac, followed by slickwater stimulation, except for stage 6 in which only a minifrac test performed. Stage 2 consisted of two (2) treatment phases, see Figure 8, due to blender mechanical issues.

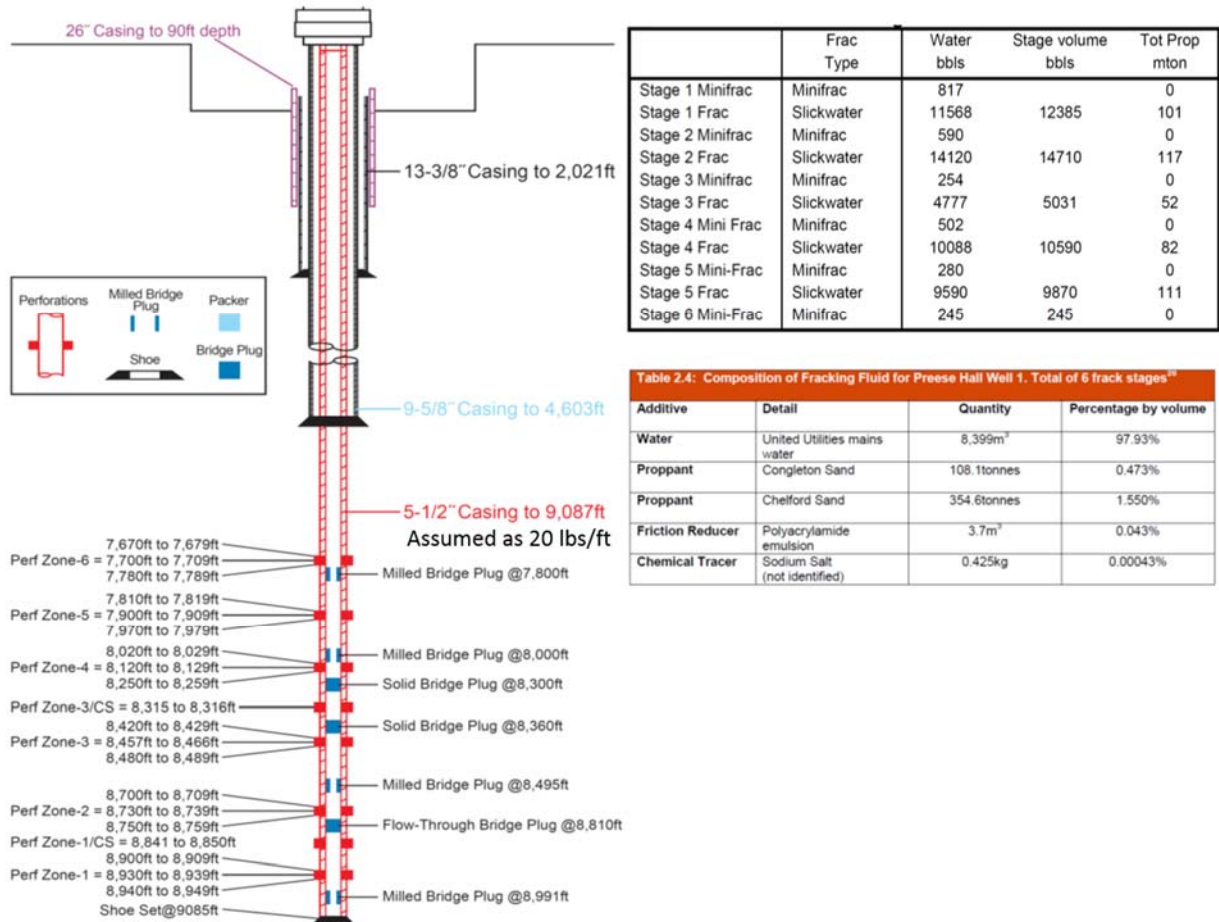


Figure 7. Presse Hall well completion with perforation zones/stimulation stages with injected fluid volumes and proppant pumped, modified from de Pater and Baisch (2011), and stimulation fluid composition taken from Broderick et al. (2011).

Following the stage 2 stimulations, an obstruction was discovered at 8,506' MD when running in a bridge plug in the 5-1/2" casing. A caliper log was run and quantified the casing deformation below this depth. The first seismic event recorded by the regional stations was during the first phase of the stage 2 stimulations was of magnitude M_L 0.5, occurring ~25 mins after WHP injections pressures rose to ~90% of the overburden pressure, as shown in Figure 8. During the second phase of the stage 2 stimulations, two events of magnitudes M_L 0.5 and M_L 1.5 also occurred ~25 mins after WHP injections pressures rose to ~90% of the overburden pressure, as shown in Figure 8. Note in this figure, the pressure plot is WHP not calculated BHP as incorrectly stated by Clarke et al. (2014).

The calculated BHPs presented in de Pater and Baisch (2011) and de Pater and Pellicer (2011) are inconsistent between treatments and were determined to be incorrect for all of the stimulation stages.

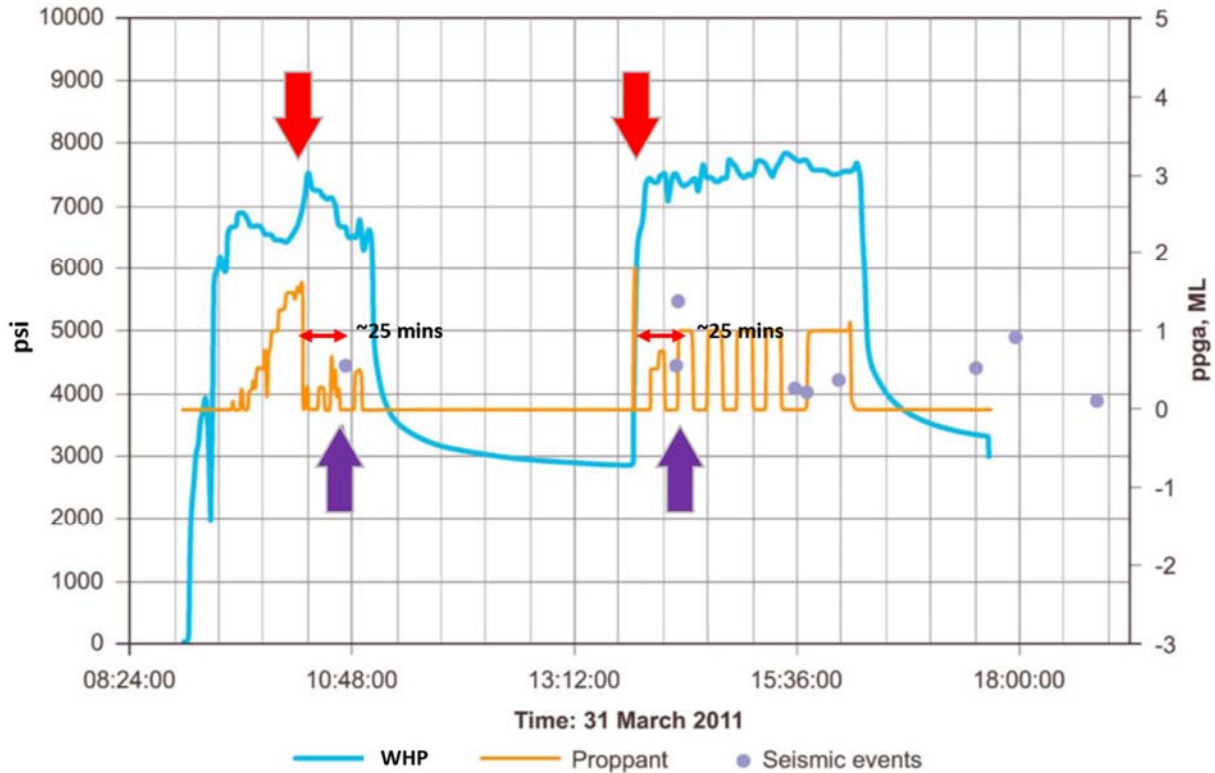


Figure 8. WHP, proppant loading and induced seismicity of the Preese Hall well Stage 2 stimulations, modified from Clarke et al. (2014), as original figure incorrectly stated that the pressures were BHP.

Thirteen (13) seismic events of magnitude $> M_L 0$. were recorded during the second phase of the stage 2 stimulations, with the largest event of $M_L 2.3$ occurring ~ten (10) hours after the well was shut in, see Figure 9.

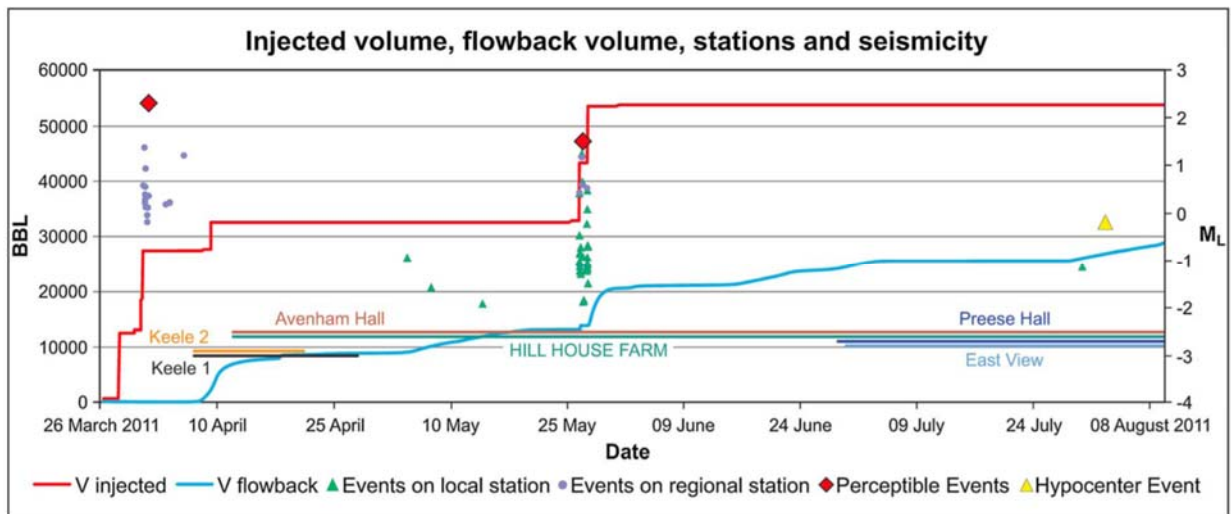


Figure 9. Injected and flowback volumes and induced seismicity of the Preese Hall well stimulations taken from Clarke et al. (2014).

Calculated BHPs reported in de Pater and Baisch (2011) were determined to be incorrect. Calculated BHPs in Baisch and Voros (2011) and Eisner et al. (2011) differed from those reported in de Pater and Baisch (2011) and although seemed closer to expected values for the stage 2 stimulations were also determined to be incorrect. BHPs that were consistent between treatments and that appeared reasonable and correct could not be found in any of the reports cited. The BHPs presented in Clarke et al. (2011) were not calculated BHPs as stated, since they were in fact measured WHPs.

Therefore, analyses were undertaken to calculate approximately what the BHPs would most likely have been during both of the stage 2 stimulations. In order to do this, some assumptions had to be made namely, a) the 5-1/2" casing weight, b) the stimulation fluid composition c) assumptions on roughness, perforations, etc. needed to be made. From these analyses the calculated BHPs in both of the stage 2 stimulations were in excess of the vertical overburden pressure throughout both treatments, and BHPs far exceeded the total normal stress on the 30° dipping slickensided bedding planes for all stimulations.

In the case of the Presse Hall well stimulations, the bedding planes were opened by the high net fracturing pressures and lead to extremely high leak-off and very low fracture fluid efficiency, both contrary to what would be required to enhance production in a nano-Darcy shale. Over the depths stimulated, a high frequency of slickensided bedding planes dipping at 30° and thin clay rich bands, parallel or subparallel to bedding, were encountered in the Preese Hall core. These features had very low frictional strength of $\phi=6^\circ$ de Pater and Baisch (2011). Both of these features impeded the vertical growth of hydraulic induced vertical fractures, that were initiated in the stiffer brittle zones by fluid injection through perforations. These hydraulic fractures vertical growth was stopped by these features, resulting in a rise of the net fracturing pressure, to allow the fracturing fluid to open and flow along the hyper-stress sensitive bedding planes, heightening the risk of induced seismicity with minimal enhanced gas production.

For example, a hydraulic induced fracture in the stiff Bowland shale under strike-slip stress state can't propagate vertically through the slickensided bedding surfaces or weak clay rich bands as detected throughout the core in the Preese Hall well stimulation depths. For measured data on stress state and strength of these slickensided bedding planes and the thin clay rich bands, validated numerical model computes that the induced hydraulic fracture will be stopped in height growth, net pressure will rise and the fracturing fluid enters and opens the hyper-stress sensitive bedding planes, yielding extreme high leak-off, high net pressures and extremely low fracture fluid efficiency – all features experienced in all of the Preese Hall stimulations.

Wireline logs of the Preese Hall well showing acoustic, compressional, density, resistivity, caliper, NPHI and gamma ray with formation and MD are shown in Figure 10 over the Bowland-Hodder shale interval. As can be seen from the gamma log there are marked changes in lithology over this interval. The only drilling event of significance recorded in this interval was stuck pipe at 7,600' MD. Drilling induced breakouts and tensile fractures were recorded and provided an assessment of the direction of the maximum principal stress, and the horizontal principal stress ratio.

The stress state is that of strike-slip, pore pressure was hydrostatic, effective stress ratios (ESR) were 0.5 and 1.3 for the σ_{h-min} and σ_{h-max} respectively, and with quantified stress states at the top of the Bowland shale, being at a MD and TVD of 6,500' were determined from minifrac, laboratory tests, and drilling induced breakouts and tensile fractures as being $\sigma_v=20$ ppg, $\sigma_{h-min}=14.3$ ppg and $\sigma_{h-max}=23.4$ ppg, with ppg (pounds per gallon) being in lbs/gal emw, and the orientation of σ_{h-max} was 173°/353°T, Baker Hughes (2011).

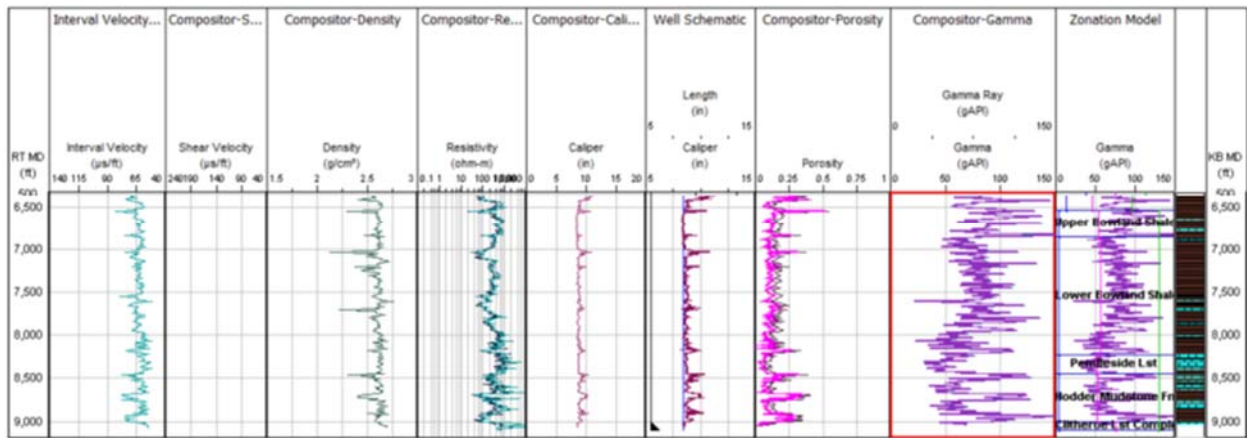


Figure 10. Wireline logs of the Bowland-Hodder shale interval in the Preese Hall well with formation and MD, adapted from Baker Hughes (2011).

A high frequency of both thin clay rich bands and slickensided bedding planes were encountered throughout the Preese Hall well. The flow of the fracturing fluid within and along these hyper-stress sensitive bedding planes maximized the risk of induced seismicity by activating the nearby fault and the resulted differential slip between the numerous calcareous/argillaceous interfaces caused the damage of the 5-1/2" casing during the stage 1 and 2 stimulations as shown in Figure 11. A high frequency of thin clay rich bands were recorded in the Hodder Mudstone formation at 8,480', 8,505', 8,560', 8,575', 8,605', 8,610', 8,620', 8,630' and 8,640' MD, and fifteen (15) slickensided bedding planes at 30° dip were recorded at measured depths greater than 8,000' MD, de Pater and Baisch (2011). Note that the slickensided bedding planes were all intersected in the Preese Hall core with a dip of 30°, see Figure 5.

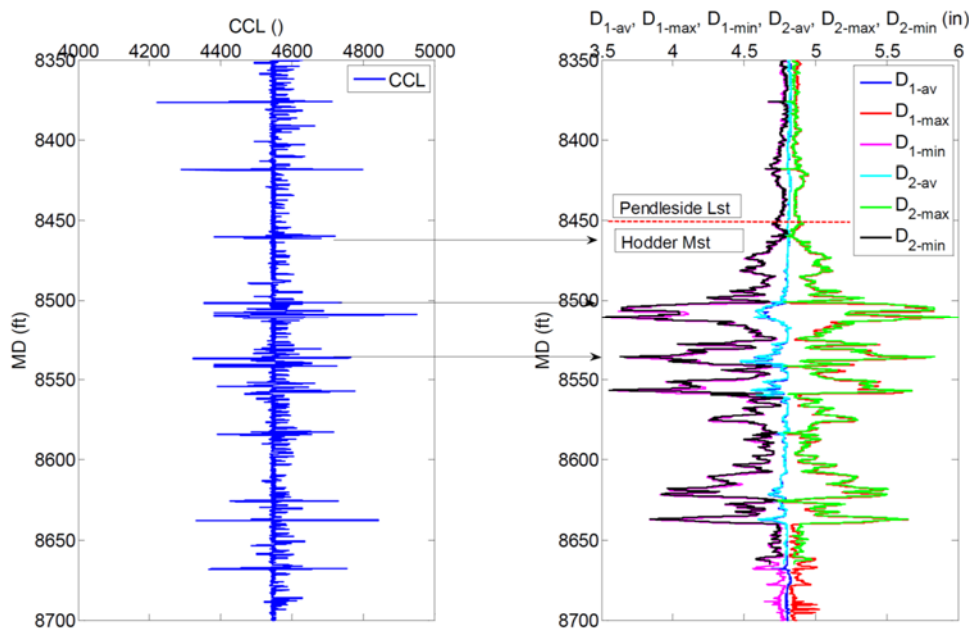


Figure 11. Preese Hall well casing deformation from 8,450' MD to 8,700' MD taken from de Pater and Baisch (2011).

From the observed drilling induced tensile fractures and breakouts, the strike-slip stress state is clearly apparent. The minifrac tests yielded high values for fracture closure pressure (σ_{h-min}) as a ratio of vertical overburden stress ranging from 0.73 to 0.96. In all cases, the minifracs computed extremely low fracture fluid efficiencies as low as ~20% in a nano-Darcy permeability shale. The low fracture fluid efficiency infers high leak-off, if the minifrac data are analyzed assuming an induced vertical hydraulic fracture orientated perpendicular to the minimum principal stress, i.e. σ_{h-min} . The minifracs induced small vertical fractures that stopped vertical growth upon reaching the weak bedding planes, the resulting high injection pressures opened the slickensided bedding planes and fluid flowed into and along the hyper-stress sensitive bedding planes. Such a scenario would account for the high leak-off and inconsistent closure stresses computed from the minifrac tests.

Table 1. Minifrac test data analysis for fracture closure pressures and ISIP, taken from de Pater and Pellicer (2011) and Baker Hughes (2011).

Table 1: Closure gradients from minifrac pressure declines. Re-analysis by StrataGen yielded much lower values in a number of cases.

Stage	Formation	TVD (ft)	TVD-SS (ft)	MD (ft)	G _{h-min} , StrataGen (psi/ft)	Pc (psi)	G _{h-min} Cuadrilla (psi/ft)
1	Lower Worston Shale	8773	8731	8896	0.73	6394	0.73
2	Mid Worston Shale	8627	8584	8730	0.837	7223	0.96
3	Upper Worston Shale	8383	8341	8455	0.77	6460	0.86
4	Lower Bowland Shale			8165	NA		0.76
5	Lower Bowland Shale	7867	7824	7895	0.79	6234	0.82
6	Lower Bowland Shale	7710	7667	7730	0.902	6926	0.95

Table 4. List of FCP and ISIP values determined from available FIT and minifrac tests. The hydraulic fracturing tests were performed using fresh water (gradient of 8.4 ppg EMW).

MD KB (ft.)	FCP GMI (PPG)	S _{hmin} Cuadrilla (PPG)	Effective stress ratio K (Low bound)	Effective stress ratio K (Upper bound)	Type of test
2,057		12.90	0.44		FIT
4,660		14.42	0.53		FIT
8,841.5 – 8,942.5	13.7	14.53 (FCP)	0.43 – 0.5	0.68	Minifrac #1
8,700.1 – 8,750.6	14.4	20.10 (ISIP)	0.49	0.98	Minifrac #2
8,420.3 – 8,480.9	13.4	18.10 (ISIP)	0.41	0.81	Minifrac #3
8,020.3 – 8,250.6	Not utilized	16.20 (ISIP)		0.66	Minifrac #4
7,810.2 – 7,970.8	15.2	18.70 (ISIP)	0.57	0.87	Minifrac #5
7,780.9 – 7,670.8	15.1	19.70 (ISIP)	0.6	0.90	Minifrac #6

The hydraulic conductivity of the bedding planes is hyper-sensitive to the effective stress. Due to this hyper-stress sensitivity of the bedding plane hydraulic conductivity to effective stress, elevated pore pressures are expected significant distances from the stimulation well. Due to the lack of data on the bedding planes, some assumptions were made based on data from similar bedding planes; namely, 1) the slickensided bedding plane wall surface material is anelastic and thus closes completely at reservoir initial conditions, 2) the bedding plane fracture fluid conductivity is highly anisotropic, with a maximum in the direction of slickensides, and 3) the bedding plane conductivity to over pressure is as shown in Figure 12, and as such the bedding plane is effectively impermeable and will not experience leak-off for an effective normal stress dimensionless ratio of >0.4 .

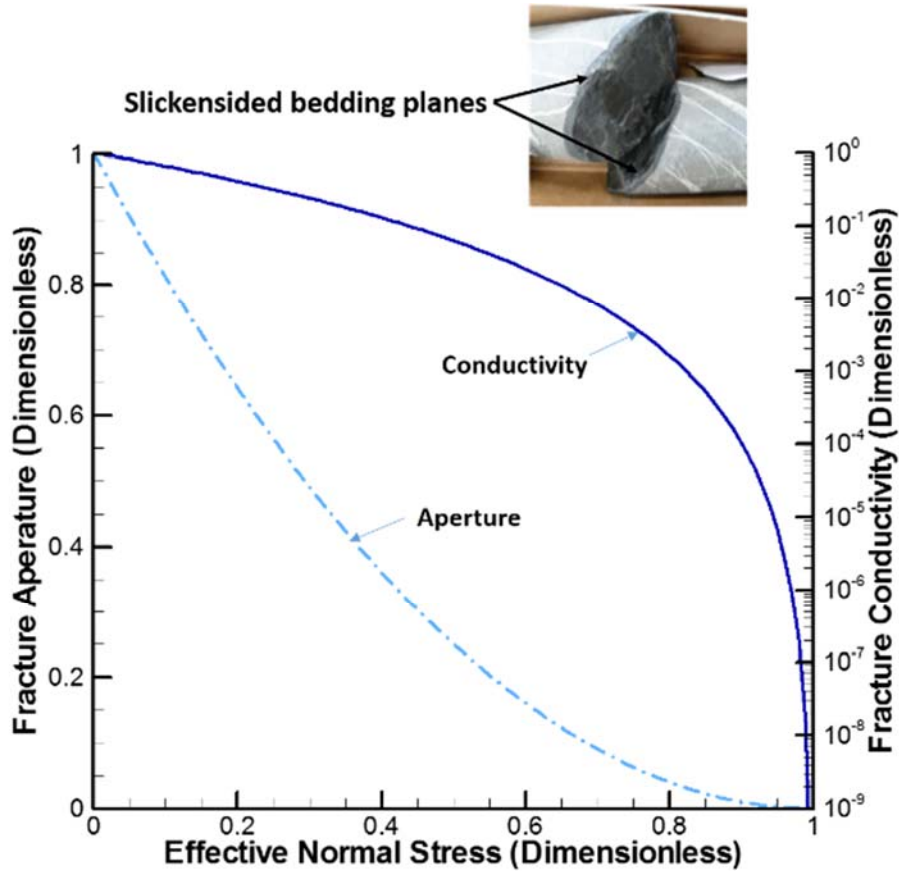


Figure 12. Assumed slickensided bedding plane fluid conductivity with effective normal stress.

The hyper-stress sensitivity fluid model calculated that significantly elevated pore pressures of $\sim 2,500$ psi occur some 1,700' away from the stimulated well with minimal time lag for the 15,000bbls of liquids injected in the Stage 2 well stimulations, as shown in Figure 13. The low pressure losses due to fluid flow along the bedding planes is a result of the overpressurizing of these planes and their hyper-sensitivity to effective stress as shown in Figure 12. A single slickenside bedding plane was assumed to be intersected in the model during the stage 2 stimulations. The number of bedding planes opened, will depend on the frequency and depth location of the slickensided bedding planes in the vicinity of initial and early propagation of the induced hydraulic fractures. The computed highly elevated pore pressures at a significant distance from the well, as shown in Figure 13, heighten the risk of induced seismicity.

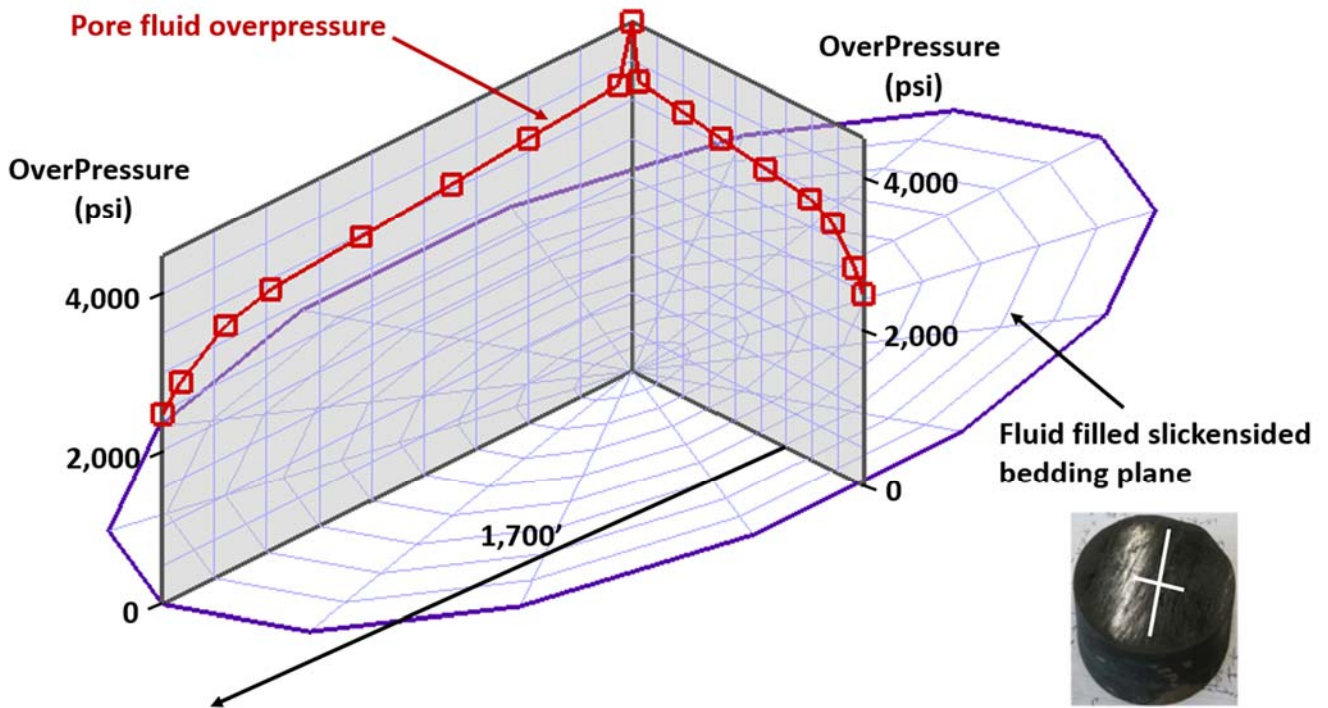


Figure 13. Opened dimensions and pore fluid overpressure on a slickensided bedding plane at the end of injection for the Stage 2 stimulations of the Preese Hall well.

During flow back of the stage 1 and 2 stimulations, the well flowed for ~4 days at a constant rate of ~750 bbls/day, i.e. at constant BHP, being pseudo-steady state, inferring a closed drainage area with a constant pressure outer boundary. Determining the fracture conductivity from flow back data and using the shutin pore fluid overpressure of the opened bedding planes of ~2,500psi, as given by Figure 13, the computed fracture conductivity was calculated to be approximately an order of magnitude drop, from that determined for injection, as per the effective stress relationship assumed in Figure 12.

The Stage 2 stimulations gave rise to a maximum induced earthquake of M_L 2.3 on 1st April, along with sixteen (16) other events greater than M_L 0, as shown in Figures 8 and 9. The hyper-stress sensitivity fluid model quantified that high shutin pressures would be experienced in the stimulation well for months to years due to the very low leakoff into the bedding planes and the formation. Such pore fluid overpressures were observed following the stimulations after shutin, and during flow back conducted ten (10) days after shutin, de Pater and Basich (2011) and de Pater and Pellicer (2011).

The stage 4 stimulations induced similar seismicity to that of the stage 2 stimulations, except that the first seismic event being of M_L 0.5 occurred ~60 mins, compared to ~25 mins after the same volume had been injected in the stage 2 stimulations. The time difference is possibly due to the stage 4 stimulations being shallower, and the fluids from the opened bedding plane had to diffuse over a greater distance to the seismic hypocenter. The largest induced seismic event of M_L 1.5 occurred ~ten (10) hours after shutin of the stage 4 stimulations, exactly the same time delay as the largest induced event of M_L 2.3 that occurred after shutin following the stage 2 stimulations.

During flow back following stage 4 and 5 stimulations, the well flowed for ~4 days at a constant rate of ~750 bbls/day, i.e. at constant BHP, being pseudo-steady state, inferring a closed drainage area with a constant pressure outer boundary, extremely similar to the flow back data following the stage 2 stimulations. Determining the fracture conductivity from flow back data and using the shutin pore fluid overpressure of the opened bedding planes of ~2,500psi, as given by Figure 13, the computed fracture conductivity was calculated to be approximately an order of magnitude drop from the injected value, as was observed following the stage 2 stimulations. This flow back data further confirms that both stimulations were similar in that they opened bedding planes some considerable distance from the stimulated well with virtually zero leak off into the formation even at moderately elevated effective normal stress.

It is due to the hyper-sensitivity of the bedding planes to stress, that such an injected fluid volume could induced seismicity some distance from the well, and it is not related to a fracture propagation rate of 4-6m/min as stated by Clarke et al. (2014). The two largest induced events of 1st April and 27th May, being M_L 2.3 and M_L 1.5 respectively, showed strong similarity of waveform on the five (5) regional stations that recorded them, constraining the relative distance between the two events as <400'. A total of fifty two (52) seismic events were recorded during and after the stimulations, all of which had similar waveforms to the two largest events of M_L 2.3 and M_L 1.5 recorded at the regional stations. The hypocenter of the major event was estimated to be ~1,200' east of the injection well, Clarke et al. (2014). The seismic data shows that in all likelihood all the induced seismic events were in close proximity to each other. The seismic data supports that elevated induced fluid pressures were felt some distance from the stimulation well as quantified by the hyper-stress sensitive fluid injection model.

The very high frequency of slickensided bedding planes and thin clay rich bands, resulted in the hydraulically induced fractures experiencing only limited height growth, resulting in a significant increase in injection pressures, with the fracturing fluid entering and opening the hyper-stress sensitive bedding planes, yielding high net pressures, high leak-off, resulting in minimal enhanced production, and providing optimum conditions for induced seismicity.

The Preese Hall stimulations demonstrate that any hydraulic induced vertical fractures that were initiated turned into and activated the extremely weak bedding planes that lead to pressurizing the neighbouring fault and caused the induced seismicity. Even if the fault was not present the stimulation of the Bowland-Hodder shales, by injecting through perforations would have produced minimal production enhancement due to the proppant placed primarily on the bedding planes.

The slickensided bedding planes and thin clay rich bands contained throughout the Bowland shale and Hodder mudstone formations, both mitigated vertical hydraulic fracture growth, resulting in an increase in injection pressures. This increase in injection pressure allowed the fracturing fluid to enter, open and flow along the existing hyper-stress sensitive bedding planes. Elevated pressures were thus experienced a significant distance from the stimulated well with minimal time lag, raising significantly the risk of induced seismicity.

From the observations, pressures and induced seismic events during and immediately after the Preese Hall well stimulations, there is an urgent need for a coherent research study to formulate a well stimulation design methodology for the Bowland-Hodder shale that ensures optimum enhanced gas production and limits the risk of induced seismicity.

Outline of Proposed Alternate Well Stimulation Method

Following the in-house review of the Preese Hall well stimulations, analyses using validated numerical models were conducted on a simplified geology to that present in the Bowland-Hodder shale interval. These preliminary analyses involved the simulation of induced vertical fractures from perforations, and calculated their propagation and interaction in the presence of the high frequency of slickensided bedding planes and thin clay rich bands. These analyses quantified that the vertical hydraulic fracture growth would be limited to their first encounter of the slickensided bedding planes or thin clay rich bands, which are parallel or subparallel to bedding. Net injection pressure subsequently rose, with BHPs calculated greater than the vertical overburden pressure, and the fracturing fluids entered and flowed along the hyper-stress sensitive bedding planes as described earlier.

Current perceived methods to achieve such a high height growth fracture at or close to the stimulated wellbore are shown in Figure 14 below, as being:

- a) complex completion of split casing and dilated expanded inner slotted liner, to initiate vertical fracture, simple pumping schedule, brute force approach, perceived as low risk,
- b) orientated slots formed by jetting or shaped charges, with the orientated slots reducing breakdown pressures, modified pumping schedule to achieve coalesced height growth of the induced hydraulic fractures, perceived as moderate risk, and
- c) orientated perforations, with complex pumping schedule to achieve multiple breakdowns with minimal fracture growth, followed by fracture growth to achieve coalesced height growth of the induced hydraulic fractures, perceived as high risk.

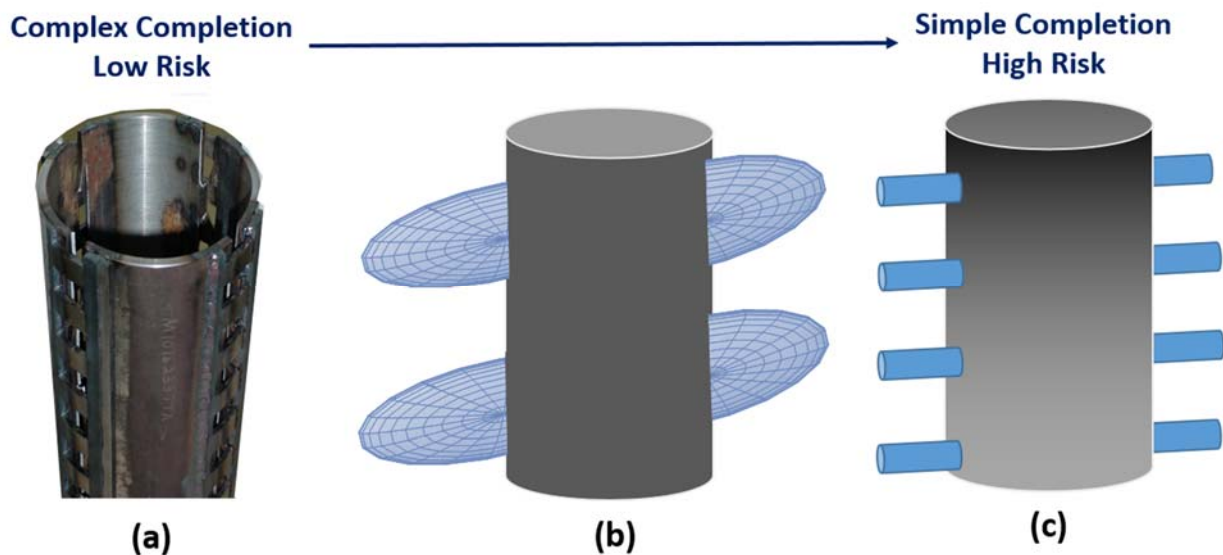


Figure 14. Current perceived stimulation methods a) sleeve initiated fracture - low risk, b) orientated slots by jetting or shape charges - moderate risk, and c) orientated perforations - high risk.

References

- Baisch, S. and R. Voros (2011). Geomechanical Study of Blackpool Seismicity, Q-Con report prepared for Cuadrilla Resources Ltd., October.
- Baker Hughes (2011). Wellbore Failure Analysis and Geomechanical Modelling in the Bowland Shales, Blackpool, UK, Baker Hughes report prepared for Cuadrilla Resources Ltd., September.
- Blanton, T. L. (1982). An Experimental Study of Interaction Between Hydraulically Induced and Pre-Existing Fractures, SPE Paper 10847, SPE/DOE Unconventional Gas Recovery Symp., Pittsburg, PA, May.
- Broderick, J., K. Anderson, R. Wood, P. Gilbert, M. Sharmina, A. Footitt, S. Glynn and F. Nicholls (2011). Shale gas: an updated assessment of environmental and climate change impacts, a report commissioned by The Co-operative and undertaken by researchers at the Tyndall Centre, University of Manchester, November.
- Clarke, H., L. Eisner, P. Styles and P. Turner (2014). Felt Seismicity Associated with Shale Gas Hydraulic Fracturing. The First Documented Example in Europe, AGU, Geophysical Research Letters, November.
- de Pater, C. J. and S. Baisch (2011). Geomechanical Study of Bowland Shale Seismicity, Synthesis Report, StratGen and Q-con report prepared for Cuadrilla Resources Ltd., November.
- de Pater, H. and M. Pellicer (2011). Geomechanical Study of Bowland Shale Seismicity, Synthesis Report, StratGen report prepared for Cuadrilla Resources Ltd., August.
- Eisner, L., E. Janska and P. Matousek (2011). Seismic Analysis of the events in the vicinity of the Presse Hall well, Seismik report prepared for Cuadrilla Resources Ltd., September.
- Eisner, L., M. Hallo, E. Janska, I. Oprsal, P. Matousek, H. Clarke, P. Turner, T. Harper and P. Styles (2013). Lessons learned from hydraulic stimulation of the Bowland Shale, SEG Technical Program, Extended Abstracts, pp4516-4520.
- Fisher, K. and N. Warpinski (2011). Hydraulic-Fracture-Growth: Real Data, SPE Paper 145949, SPE Annual Tech. Conf. & Exhibit, Denver, CO., October-November.
- Gale, J. F. W., R. M. Reed and J. Holder (2007). Natural Fractures in the Barnett Shale and their importance for hydraulic treatments, AAPG Bull., 91, 4, pp603-622.
- Green, C. A., P. Styles and B. J. Baptie (2012). Preese Hall Shale Gas Fracturing, Review and Recommendations for Induced Seismic Mitigation, report prepared for the UK DECC, April.
- Hocking, G., T. W. Cavender, J. Person and T. Hunter (2012). Single-Well SAGD Field Installation and Functionality Trials, SPE Paper 157739, SPE Heavy Oil Conference Canada, Calgary, AB, June.
- Hocking, G., T. W. Cavender, T. Hunter and G. Li (2013). Comparisons of Plane Propagation from Dilating Casing and Conventional Perforations when Stimulating the Milk River Formation, 47th US Rock Mechanics Geomechanics Symp., San Francisco, CA, June.
- Warpinski, N. R., L. D. Tyler, W. C. Vollendorf and D. A. Northrop (1981). Direct Observations of a Sand Propped Fracture, Sandia National Laboratories, Report No SAND81-0255, Albuquerque, New Mexico, May.